SPE
Society of Petroleum Engineers of AIME

SPE 12267

Incorporation of Mixed Finite Element Methods in Compositional Simulation for Reduction of Numerical Dispersion

by R.E. Ewing, *U. of Wyoming,* and R.F. Heinemann, *Mobil R&D Corp.*

Members SPE-AIME

This paper was presented at the Reservoir Simulation Symposium held in San Francisco, CA, November 15–18, 1983. The material is subject to correction by the author. Permission to copy is restricted to an abstract of not more than 300 words. Write SPE, 6200 North Central Expressway, Drawer 64706, Dallas, Texas 75206 USA. Telex 730989 SPEDAL.

ABSTRACT

Previous studies have shown that standard finite difference techniques cause numerical dispersion and grid orientation problems when used to simulate enhanced recovery processes with adverse mobility ratios. In compositional simulation, numerical dispersion can diffuse sharp fluid interfaces yielding erroneous predictions of fluid compositions and corresponding errors in the velocities of the miscible frontal advance. Numerical dispersion can also effect the computed locations of the boundaries of the regions of single-phase and two-phase flow.

Inaccurate fluid velocities and suboptimal use of upstream weighting of transport terms combine to cause many aspects of the numerical dispersion and grid orientation problems. A mixed finite element method has been developed to obtain more accurate approximations to the fluid velocities. In this method the Darcy velocities are considered as primary variables together with the total fluid pressure.

Although finite element techniques are used to compute the more accurate fluid velocities, these velocities are then incorporated into a more standard finite difference method for the bulk of the simulation process. This paper presents the use of mixed methods in a two-dimensional finite difference compositional simulator to reduce problems caused by numerical dispersion. Comparisons are made with a standard finite difference simulator on problems involving immiscible displacement and multiple contact miscibility phenomena.

INTRODUCTION

Compositional reservoir models are receiving considerable attention since they are applicable to enhanced recovery techniques such as CO_2 injection into oil reservoirs and to the primary depletion or N_2 injection into gas condensate reservoirs. These processes are distinct, from the mathematical modelling point of view, since the distribution and properties of the reservoir fluids depend on both pressure and composition. Compositional simulators account for this distinction by treating the oil and gas phases as multi-component mixtures and tracking the compositions of the individual phases by using equations which describe phase equilibrium and species mass conservation. Accuracy of the recovery estimates produced by these models ultimately depend on the computed saturation, pressure, and composition profiles.

Several formulations of field scale, compositional simulators have appeared in the literature [1-6], and the objective here is not to expand this list but rather to discuss the effect of the discretization technique on the solution profiles. Most of the current formulations employ finite differences with upstream weighting to discretize the flow equations. Use of this discretization creates errors which tend to smooth sharp composition and saturation gradients that are expected when modelling enhanced oil recovery processes. These errors are commonly referred to as numerical dispersion. Coats [4] has previously illustrated this effect in one dimension by solving a multiple contact miscible problem with a varying number of grid blocks. His results show that the location of the two-phase region and the miscible front, the concentration profiles, and the hydrocarbon recovery were all affected to some degree by the number of blocks used in different runs.

While Coats did not offer a remedy for controlling the numerical dispersion, several methods that are potentially applicable to compositional models have been proposed [7-8]. These techniques attempt to obtain a cancellation of the spatial and time truncation errors but their effectiveness is not clear for multi-dimensional problems. Nolen [1] has reported some success in controlling dispersion with the method of characteristics.

The goal of this work is the development of a procedure for reducing numerical dispersion in a compositional setting. Our proposed scheme uses standard finite differences to solve a discretized pressure equation and then employs a type of mixed finite element method to solve for phase velocities. These velocities are used in the explicit computation of the remaining composition variables. The mixed method velocities are considerably more

References and illustrations at end of paper.

accurate than those produced by differencing the pressure in Darcy's law and exhibit a marked effect on the computed saturation and composition profiles.

Our use of a mixed method is motivated by its success in eliminating numerical dispersion and grid orientation for immiscible displacement [9] and first-contact, miscible displacement [10, 11] problems. In these settings, mixed methods have been used to solve for the Darcy velocity of the total fluid. By solving for the total velocity as one term, difficulties occurring in standard methods caused by differencing or differentiating a computed approximation to the pressure, and then multiplying by rapidly changing coefficients, were minimized. The total fluid velocity is a relatively smooth function of space, changing sharply in the neighborhoods of wells. This is because local changes in the total fluid pressure compensate for rapid variation in permeability, resulting in a smooth fluid velocity. The use of the velocity as a primary variable added both accuracy and robustness to the computations described in References 10 and 11.

In the compositional setting several species are present and different phases compete for flow through the reservoir. The total fluid velocity is not sufficient to describe the flow processes, and phase velocities must be determined separately. In our methods a total velocity is first determined, and then finite element techniques are used to apportion the velocity to the separate phases without the use of upstream weighting. As the number of phases present in the reservoir changes, the relative permeabilities may vary rapidly with the saturations. This rapid change in relative permeabilities enhances the difficulties caused by upstream weighting techniques. This weighting treats upstream flow between adjacent grid blocks with relative permeabilities 1 and 0 exactly the same as if the relative permeabilities were 1 and 1, hence forcing too much fluid to flow and diffusing sharp fluid interfaces.

We shall next present the mathematical model which is used for our test simulations and discuss standard finite difference solution techniques. We describe the form of the mixed method used and its implementation. Then we present test simulations for both immiscible and miscible displacement with three hydrocarbon components and water present. The computational results demonstrate that the use of finite element phase velocities reduce the numerical dispersion of the gas saturation and composition profiles, maintaining sharper fluid interfaces.

MATHEMATICAL MODEL

The mathematical model discussed here describes the flow of N hydrocarbon species which comprise the oil, gas, and water phases in porous media. The mass balances in the model are derived from the species continuity equations for each hydrocarbon component and water:

$$(1)\quad \phi \frac{\partial(\rho_o S_o + \rho_g S_g)\, z_i}{\partial t} = - \nabla \cdot (\rho_o x_i V_o + \rho_g y_i V_g) + q_i, \quad i=1, \ldots N,$$

$$(2)\quad \phi \frac{\partial \rho_w S_w}{\partial t} = - \nabla \cdot \rho_w V_w + q_w .$$

In several compositional formulations, it has been convenient to sum the N equations represented in (1) to form an overall hydrocarbon balance which is often used to solve for pressure:

$$(3)\quad \phi \frac{\partial \alpha}{\partial t} = - \nabla \cdot (\rho_o V_o + \rho_g V_g) + q ,$$

where

$$(4)\quad \alpha = \rho_o S_o + \rho_g S_g .$$

The phase velocities in equations (1) to (3) are related to the reservoir pressure by Darcy's law. Neglecting capillary pressure and gravity forces, the oil velocity is expressed as

$$(5)\quad V_o = - \frac{k k_{ro}}{\mu_o} \nabla P .$$

We also assume that thermodynamic equilibrium exists between the hydrocarbon phases, and this equilibrium is expressed in a set of N constraints requiring that the oil and gas fugacities be equal for each component,

$$(6)\quad f_{io} = f_{ig} , \qquad i=1, \ldots N.$$

We have employed the Peng-Robinson equation of state [12]

$$(7)\quad z^3 - (1 - B)z^2 - (A - 3B^2 - 2B)z - (AB - B^2 - B^3) = 0$$

to derive the following equation

$$(8)\quad \ln \frac{f_i}{x_i P} = \frac{b_i}{b}(z - 1) - \ln(z - B) - \frac{A}{2\sqrt{2}\,B}\left(\frac{2\sum_j x_j a_{ij}}{a} - \frac{b_i}{b}\right) \ln \frac{z + 2.414\,B}{z - 2.414\,B}$$

from which the fugacity may be computed. The mathematical model is completed by requiring that the phase saturations sum to unity

$$(9)\quad S_o + S_g + S_w = 1 .$$

FINITE DIFFERENCE REPRESENTATION

The derivative operators in the model equations can be discretized by applying the usual finite difference analogues. The overall hydrocarbon equation in two dimensions then becomes

$$(10)\quad \phi_{i,j} \frac{(\alpha_{i,j}^{n+1} - \alpha_{i,j}^{n})}{\Delta t} = - \left(\frac{\rho_o V_{o\ i+1/2,j}^{n+1} - \rho_o V_{o\ i-1/2,j}^{n+1}}{\Delta x}\right) - \left(\frac{\rho_o V_{o\ i,j+1/2}^{n+1} - \rho_o V_{o\ i,j-1/2}^{n+1}}{\Delta y}\right) - \left(\frac{\rho_g V_{g\ i+1/2,j}^{n+1} - \rho_g V_{g\ i-1/2,j}^{n+1}}{\Delta x}\right) - \left(\frac{\rho_g V_{g\ i,j+1/2}^{n+1} - \rho_g V_{g\ i,j-1/2}^{n+1}}{\Delta y}\right) + q_{i,j}.$$

Darcy's law can be rewritten in a similar fashion to express the phase velocities V_o and V_g as

$$(11)\quad V_{o\ i+1/2,j}^{n+1} = - \frac{k_{i+1/2,j}^{n}\, k_{ro\ i+1/2,j}^{n}}{\mu_{o\ i+1/2,j}^{n}} \left(\frac{p_{i+1,j}^{n+1} - p_{i,j}^{n+1}}{\Delta x}\right)$$

and

$$(12)\quad V_{g\ i+1/2,j}^{n+1} = - \frac{k_{i+1/2,j}^{n}\, k_{rg\ i+1/2,j}^{n}}{\mu_{g\ i+1/2,j}^{n}} \left(\frac{p_{i+1,j}^{n+1} - p_{i,j}^{n+1}}{\Delta x}\right) .$$

The next step in this procedure is usually to substitute (11) and (12) into (1) and (10) to eliminate the phase velocities and express the flow equations in terms of pressure. The resulting equations still require the evaluation of the interblock flow variables such as relative permeability at points midway between the centers of adjacent grid blocks as noted in (11) and (12). The spatial accuracy of the finite difference representation depends on the evaluation of the interblock terms via an averaging or upstream weighting. If these interblock terms do not change rapidly between blocks, upstream weighting will be fairly accurate as well as robust. However, one must exert care with weighting strategies with rapidly varying coefficients in (11) and (12). Our test results indicate the effect of different weighting methods for these terms on the computed solution profiles.

MIXED FINITE ELEMENT METHOD

In our scheme, we treat the velocities as primary unknowns and use a type of mixed finite element method to compute the velocities at the locations on the cell boundaries required by (10)-(12). Through the finite element implementation, the values of the coefficients from (11) and (12) are weighted in a manner which more accurately describes the true flow. This results in lower phase velocities at the fluid interfaces and helps to maintain a better frontal resolution.

We begin our mixed method computations by approximating the total fluid velocity. Let

$$(13)\quad \lambda_T = \frac{k k_{ro}}{\mu_o} + \frac{k k_{rg}}{\mu_g} + \frac{k k_{rw}}{\mu_w}$$

denote our total fluid mobility, and define the total velocity by

$$(14)\quad V_T = - \lambda_T \nabla P .$$

The spatial variation of the total mobility is gradual; as k_{ri} for one species goes to zero the others rise in a compensatory fashion. A variety of techniques can be used to approximate V_T, including upstream weighting or the mixed finite element methods described elsewhere in some detail in References 9-11 and 13.

Once an approximation to V_T is obtained, the phase velocities can be computed via finite element methods in a very inexpensive fashion. For example, multiplying both sides of (3) by a smooth test function χ and integrating over the reservoir (denoted by Ω), we obtain

$$(15)\quad \iint_\Omega V_o\, \chi\, dxdy = - \iint_\Omega \frac{k k_{ro}}{\mu} \nabla P\, \chi\, dxdy .$$

Then, substituting (14) into (15) yields

$$(16)\quad \iint_\Omega V_o\, \chi\, dxdy = \iint_\Omega \frac{k k_{ro}/\mu}{\lambda_T} V_T\, \chi\, dxdy .$$

We see that the phase velocity is obtained from the total fluid velocity by apportioning the phase mobility via a finite element method. The integral appearing in (16) allows the use of as much functional information on the interblock coefficients as is available via a proper choice of quadrature rule. If, as in the present situation, these terms are only known as constants on each grid block, then these terms can be pulled out of the local integrals of the finite element method as constants. Care must be taken when some relative phase permeabilities are zero in inverting the matrix to solve (16).

The pressures are considered as piecewise constant functions on the grid blocks in (14). The finite element spaces for velocities are also defined locally on each grid block. The x-component of the velocities are the tensor product of continuous piecewise linear functions in x and constant functions in y while the y-component of the velocities are tensor products of constant functions of x and continuous piecewise linear functions of y. On a rectangular computational grid, the usual no-flow boundary conditions are enforced by specifying zero functional boundary conditions on sides with x = constant for the x-component of the velocity and zero boundary conditions on sides with y = constant for the y-component of the velocity.

For a more detailed description of these function spaces, see References 13 and 14. The matrices arising from using these spaces in (15) are tridiagonal matrices for the two-dimensional problems considered in this paper and are thus very easy to invert. For theoretical convergence results for the use of mixed finite element methods in a first-contact miscibility setting, see References 15 and 16.

DISCUSSION OF RESULTS

In this section, we compare the computational results for two problems using the finite difference method with upstream weighting and with mixed method velocities. Gas was injected in both problems into a three-component oil with an initial composition of 44% methane, 12% butane, and 44% decane. The reservoir was initially at 1880 psi and 160°F with a porosity of 15% and a permeability of 100 md. The bubble point pressure of the in-place fluid was 1854 psi and the water saturation was set to its irreducible value of 22%. The problem was configured as a one quarter, five spot with a constant production rate of 22,500 lbmoles/day and a constant injection rate of 25,000 lbmoles/day.

The composition of the injection gas in the first problem was 100% methane which rapidly raised the bubble-point pressure and created an expanding region of two phase flow. Due to the pressures generated in this problem and the phase behavior of the methane-butane-decane system, multiple contact

miscibility can not be achieved [17]. Hydrocarbon recovery was due to an immiscible gas displacement.

We produce comparisons between upstream weighting and finite element weighting for this problem at 25 days, 75 days, and 125 days. Our results show how the gas interface travels across the reservoir in time and fingers into the production well. At 25 days we can see that the gas saturation profile was clearly more diffuse for the finite difference case. Figure 1 also indicates that although the edge of the two phase region (approximated by the 0.05 saturation contour) for the two methods appeared to be essentially the same, the contour lines for the finite element case are closer together, illustrating a more nearly frontal behavior. The 0.45 saturation contour lines produced by the two methods are drastically different. Since the finite element method does not disperse the fluid as rapidly as with upstream weighting, methane builds up behind the front, and thus the 0.45 Sg contour has moved much farther into the domain than with finite differences. Figure 2 presents the methane composition profile across the diagonal of the reservoir.

The results shown in Figure 3 illustrate a similar but more exaggerated difference than those in Figure 1. We again see that the 0.45 contour extends much farther into the reservoir for the mixed method, and the front generated by the finite element weighting is much sharper. Figure 4 compares the computed methane profiles and shows the severe smearing of the front caused by upstream weighting.

After 125 days the differences in the simulation results illustrated in Figure 5 are dramatic. The fingering flow into the well is very pronounced in the case of finite element weighting and noticeable only in the 0.2 S_g contour in the upstream weighted case. The leading tip of the 0.55 contour for the standard case has advanced about 20% of the distance from the injector to the producer, while the new weighting moves this tip about 70% of the diagonal distance. It can also be noted that the increased fingering in the finite element case concentrates the methane along the diagonal flow path between the wells. Figures 2, 4, and 6 indicate that the methane mole fraction at the producer is lower for the finite element computations which account for the increased methane concentrations away from the well.

The second problem is identical to the first problem except the composition of the injection gas is changed to 70% methane and 30% butane. This mixture composition enables the injection gas to become miscible with the in-place fluid via a multiple contact mechanism [17]. Our results show the usual phase transitions from a single phase liquid to a gas and oil mixture to a single phase miscible fluid as we move from the producer back to the injector. We again compared our discretization schemes for this problem and found that the location and propagation rates of both the miscible and two-phase regions and the saturation contours were all affected by the type of mobility weighting employed.

In Figure 7 we note that, after 170 days the size of the miscible region (and thus its speed of propagation) was larger if finite element mobility weighting was used. As in the immiscible regime, with mixed method velocities the contour lines were also somewhat closer together, indicating a sharper gas front, and possessed a tendency to finger toward the production well. The effect of grid orientation problems is also in evidence. We believe the oscillation of the 0.15 S_g contour is caused by these orientation difficulties which allow too much fluid to flow down the sides of the reservoir. This also allows gas to flow back toward the production well and causes non-physical curvature of the saturation contours. This problem is not apparent in the saturation profiles obtained with upstream mobility weighting. The increased sharpness of the gas front and the tendency, in the finite element case, to finger into the well are even more apparent at 265 days as indicated by Figure 8. The 0.2 contour now exhibits the spatial oscillation caused by grid orientation and exasperated by the inability of our admittedly coarse grid (5 x 5) to resolve sharp interfaces.

We also note comparisons of the speed of propagation of the miscible front for this problem. Both Figures 7 and 8 illustrate that the mixed method computations move this front ahead of the front predicted by the upstream weighting. Additional computations show that the finite difference results require about 20-25 days to reach the location of the 0.78 contour produced by the finite element weighting at 170 days and well over 30 days to reach this contour at 265 days. This qualitatively agrees with Coats' predictions of the miscible front location with varying grid sizes [4].

CONCLUSIONS

The use of phase velocities, obtained via a mixed finite element formulation, in a finite difference setting appears to possess potential for reservoir modelling. In limited test simulations for both immiscible and miscible flow regimes, the finite element weighting of mobilities produces sharper fluid interfaces and more marked fingering behavior than standard upstream weighting techniques. The finite element methods predict a more rapid advance of miscible fronts and different locations of multiphase boundaries.

Although numerical dispersion seems to be reduced by the use of finite element velocities, grid orientation problems are still present in our simulation results.

As sharper interfaces are predicted, the coarse grid spacings used in many simulators may not be adequate to resolve the fronts. Capabilities for local, spatial refinement should become important for simulation of sharp interfaces in a field scale model.

NOMENCLATURE

a, b - parameters for Peng-Robinson equation of state

A, B - parameters for Peng-Robinson equation of state

f_{ig}, f_{io} - fugacities, psi

k - permeability of the reservoir, md

k_{ro}, k_{rg}, k_{rw} - relative permeabilities, dimensionless

n - time level

N - number of hydrocarbon components

P - total fluid pressure, psi

q_i, q_w - mass flow rates at the wells, moles/ft^{3}D

S_o, S_g, S_w - saturations of oil, gas, and water, dimensionless

t - time, days

V_o, V_g, V_w - Darcy velocities for oil, gas, and water, ft/D

V_T - total fluid velocity, ft/D

x_i, y_i, z_i - mole fractions, dimensionless

Δt - time discretization level, days

Δx, Δy - spatial discretization level, ft

α - overall hydrocarbon density, moles/ft^3

λ_T - total fluid mobility, md/cp

μ_o, μ_g, μ_w - phase viscosities, cp

ρ_o, ρ_g, ρ_w - densities of oil, gas, and water, moles/ft^3

ϕ - porosity of the reservoir, dimensionless

χ - test function for velocity equation

Ω - spatial domain for the reservoir, ft^2

SI METRIC CONVERSION FACTORS

cp	x	1.0	E - 03	=	Pa • s
ft^3	x	2.831	E - 02	=	m^3
ft	x	3.048	E - 01	=	m
md	x	9.869	E - 16	=	m^2
psi	x	6.894	E + 00	=	kPa
°F		(°F - 32)/1.8		=	°C

ACKNOWLEDGMENTS

The authors are grateful to Mobil Research and Development Corporation for permission to publish this paper. The authors would also like to thank Dr. Aziz Odeh and Professor Mary Wheeler for many valuable discussions.

REFERENCES

1. Nolen, J. S., "Numerical Simulation of Compositional Phenomena in Petroleum Reservoir," Reprint Series No. 11, Numerical Simulation, Society of Petroleum Engineers of AIME, Dallas (1973), 269-284.

2. Kazemi, H., Vestal, C. R., and Shank, G. D., "An Efficient Multicomponent Numerical Simulator," Soc. of Pet. Eng. J. (October 1978), 355-368.

3. Fussell, L. T. and Fussell, D. D., "An Iterative Technique for Compositional Reservoir Models," Soc. of Pet. Eng. J. (August 1979), 211-220.

4. Coats, K. H., "An Equation of State Compositional Model," Soc. of Pet. Eng. J. (October 1980), 363-376.

5. Nghiem, L. X., Fong, D. K., and Aziz, K., "Compositional Modeling with an Equation of State, Soc. of Pet. Eng. J. (December 1981), 687-698.

6. Young, L. C., and Stephensen, R. E., "A Generalized Compositional Approach for Reservoir Simulation," Society of Petroleum Engineers of AIME 10516, 6th SPE Symp. on Reservoir Simulation, New Orleans (1982), 405-429.

7. Chaudhari, N. M., "An Improved Numerical Technique for Solving Multidimensional Miscible Displacement, Soc. of Pet. Eng. J. (September 1971), 277-284.

8. Laumbach, D. D., "A High Accuracy Finite-Difference Technique for Treating the Convection-Diffusion Equation," Society of Petroleum Engineers of AIME 3996, (December 1975), 517-531.

9. Chavent, G., Jaffre, J., Cohen, G., and Dupuy, M., "Simulation of Two-Dimensional Waterflooding using Mixed Finite Elements," Society of Petroleum Engineers of AIME 10502, 6th SPE Symp. on Reservoir Simulation, New Orleans (1982), 147-158.

10. Darlow, B. L., Ewing, R. E., and Wheeler, M. F., "Mixed Finite Element Methods for Miscible Displacement in Porous Media," Society of Petroleum Engineers of AIME 10501, 6th SPE Symp. on Reservoir Simulation, New Orleans (1982), 137-145.

11. Ewing, R. E., Russell, T. F., and Wheeler, M. F., "Simulation of Miscible Displacement Using Mixed Methods and a Modified Method of Characteristics," Society of Petroleum Engineers of AIME 12241, 7th SPE Symp. on Reservoir Simulation, San Francisco (1983).

12. Peng, D. Y., and Robinson, D. B., "A New Two-Constant Equation of State, "Ind. Eng. Chem. Fundam. Vol. 15 (1976), 59-64.

13. Ewing, R. E., and Wheeler, M. F., "Computational Aspects of Mixed Finite Element Methods," Numerical Methods for Scientific Computing, R. S. Stepleman, ed., North Holland Publ. Co. (to appear).

14. Schultz, M. H., Spline Analysis, Prentice-Hall, 1972.

15. Douglas, J., Jr., Ewing, R. E., and Wheeler, M. F., "The Approximation of the Pressure by a Mixed Method in the Simulation of Miscible Displacement," R.A.I.R.O. Analyse Numérique 17 (1983), 17-34.

16. Douglas, Jr., Jr., Ewing, R. E., and Wheeler, M. F., "Time-Stepping Methods for Simulation of Miscible Displacement Using Mixed Methods for Pressure Approximation," R.A.I,R.O. Analyse Numérique (to appear).

17. Hutchinson, C. A., Jr., and Braun, P. H., "Phase Relations of Miscible Displacement in Oil Recovery," A.I.Ch.E. Journal (March 1961), Vol. 7, 64-72.

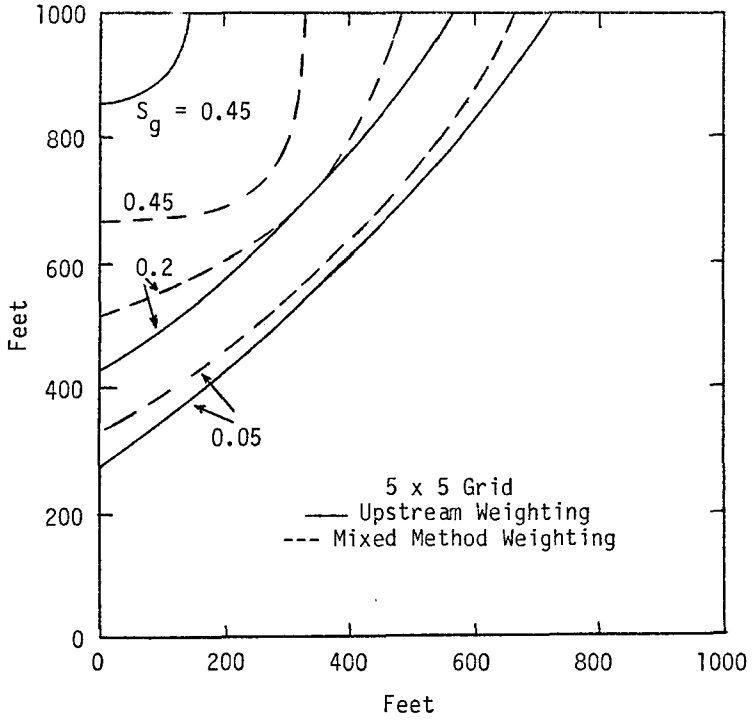

Figure 1 - Gas Saturation Contours at 25 Days

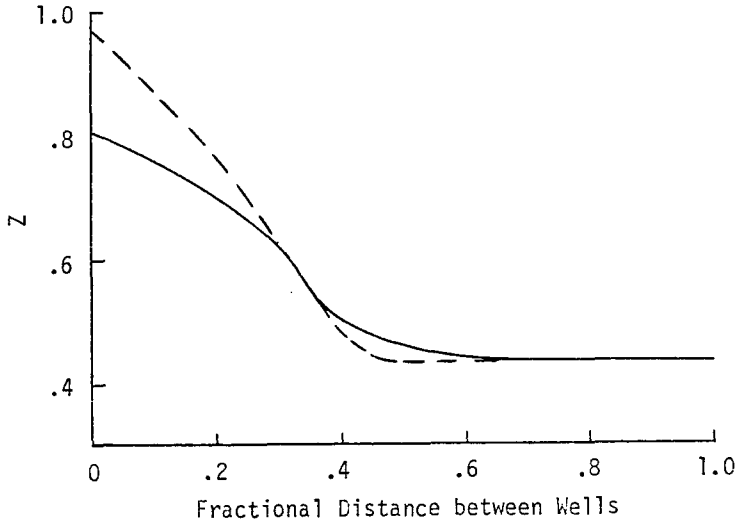

Figure 2 - Methane Mole Fraction along the Diagonal between Wells at 25 Days

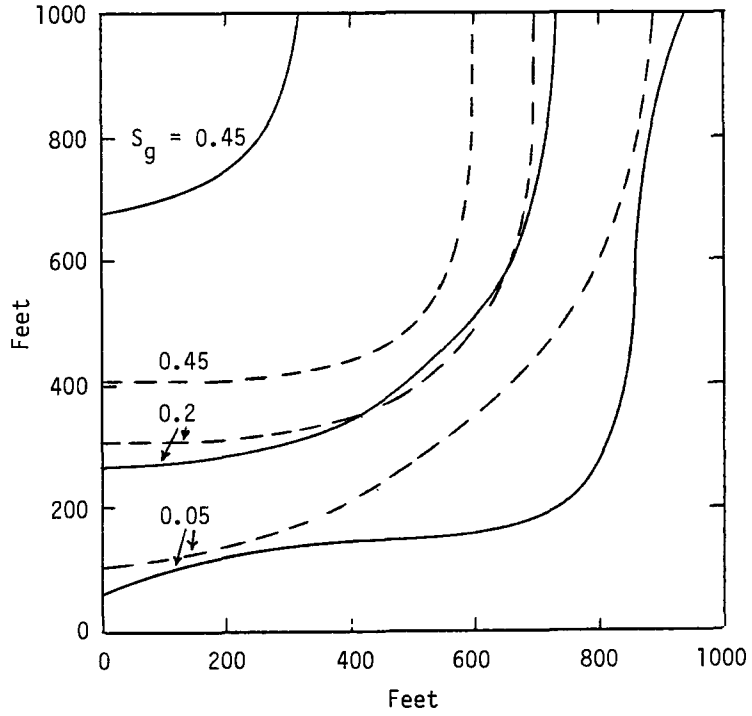

Figure 3 - Gas Saturation Contours at 75 Days

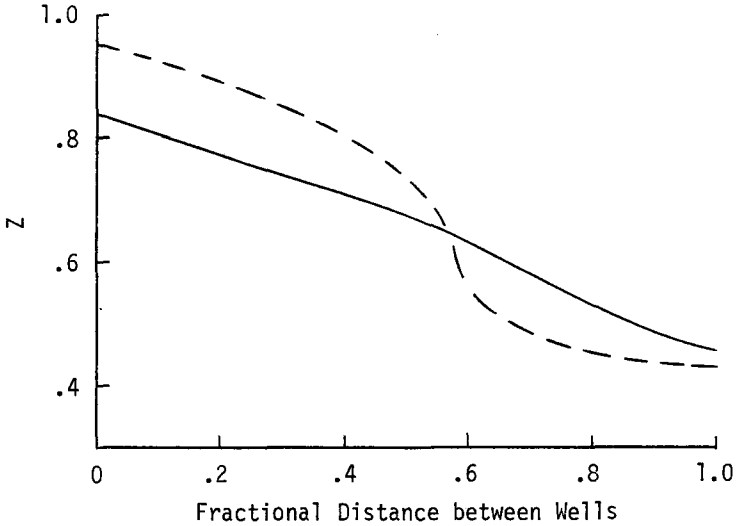

Figure 4 - Methane Mole Fraction along the Diagonal between Wells at 75 Days

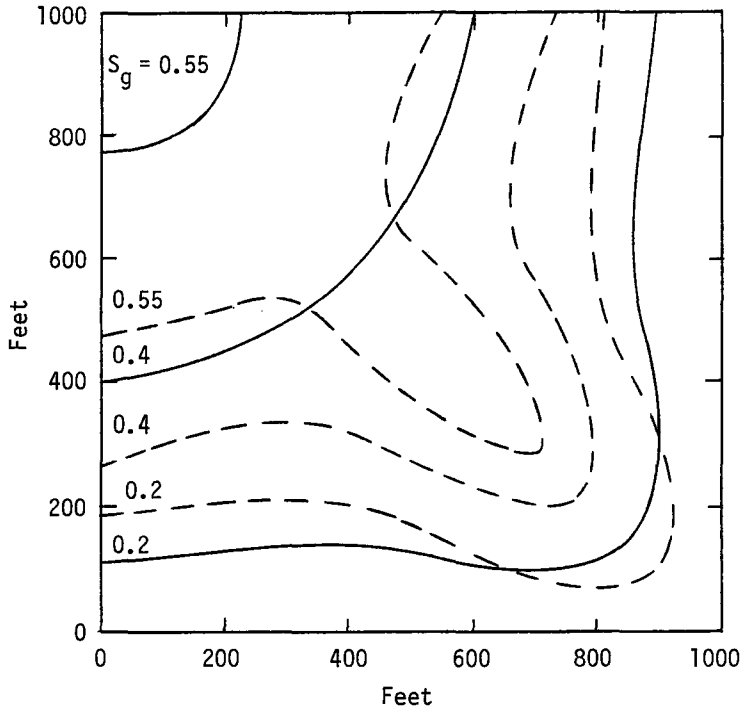

Figure 5 - Gas Saturation Contours at 125 Days

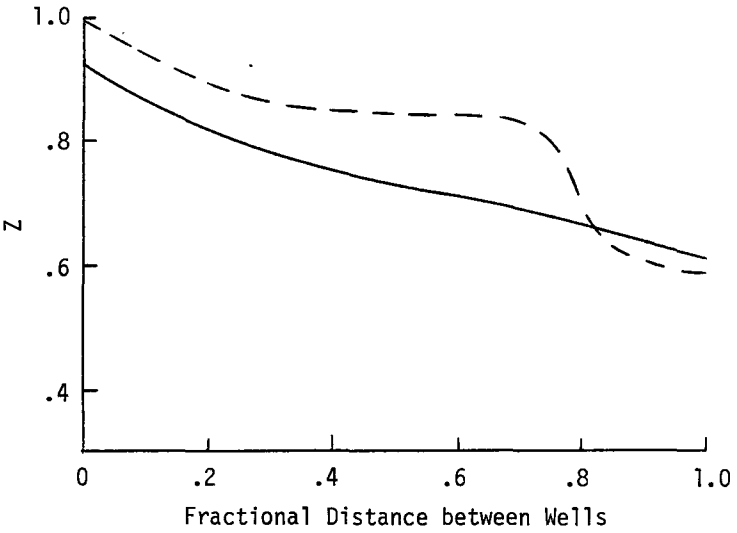

Figure 6 - Methane Mole Fraction along the Diagonal between Wells at 125 Days

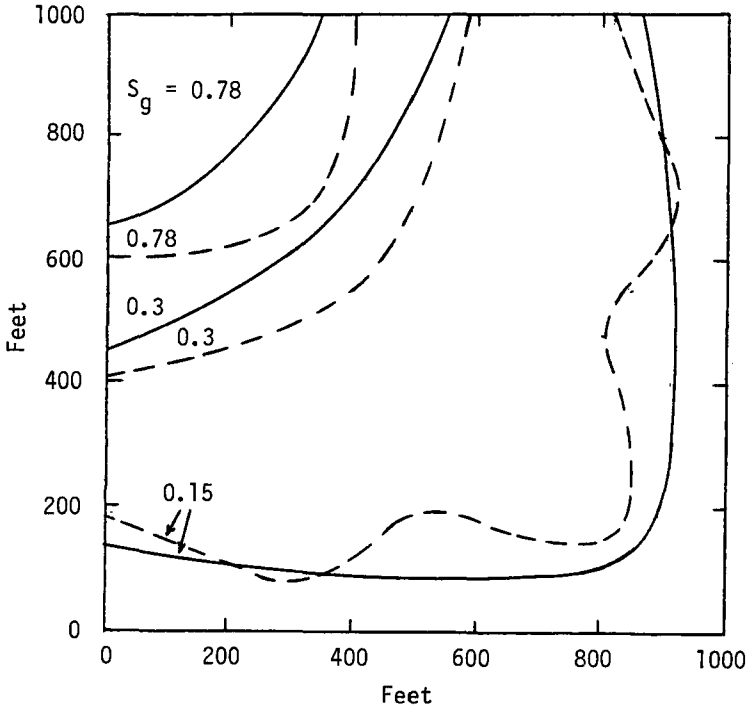

Figure 7 - Gas Saturation Contours for Miscible Displacement at 170 Days

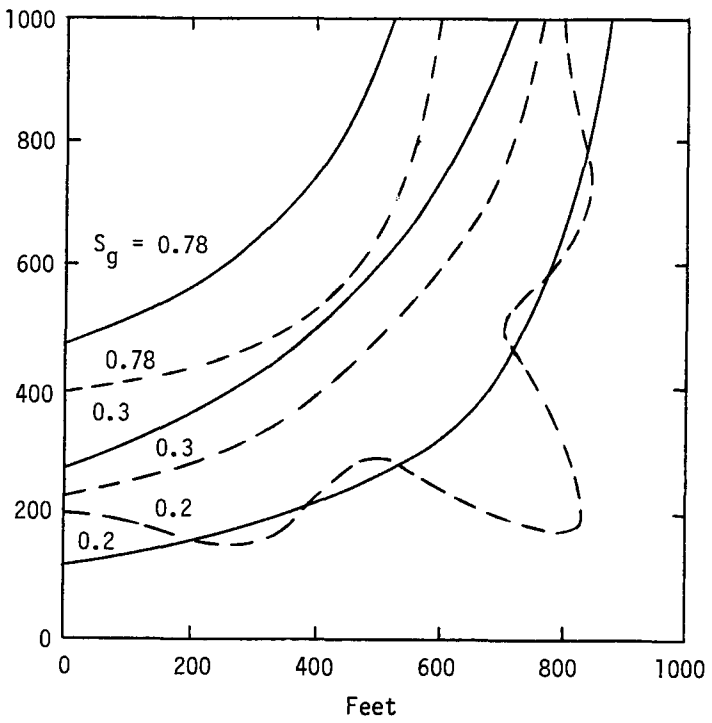

Figure 8 - Gas Saturation Contours for Miscible Displacement at 265 Days